ACADEMIC
PRESS

An analytical particle damping model

Steven E. Olson*

University of Dayton Research Institute, 300 College Park, Dayton, OH 45469, USA

Abstract

Particle damping is a passive vibration control technique where multiple auxiliary masses are placed in a cavity attached to a vibrating structure. The behavior of the particle damper is highly non-linear and energy dissipation, or damping, is derived from a combination of loss mechanisms. These loss mechanisms involve complex physical processes and cannot be analyzed reliably using current models. As a result, previous particle damper designs have been based on trial-and-error experimentation. This paper presents a mathematical model that allows particle damper designs to be evaluated analytically. The model utilizes the particle dynamics method and captures the complex physics involved in particle damping, including frictional contact interactions and energy dissipation due to viscoelasticity of the particle material. Model predictions are shown to compare well with test data.
© 2003 Elsevier Science Ltd. All rights reserved.

1. Introduction

Active and passive damping techniques are common methods of attenuating the resonant vibrations excited in a structure. Active damping techniques are not applicable under all circumstances due, for example, to power requirements, cost, environment, etc. Under such circumstances, passive damping techniques are a viable alternative. Various forms of passive damping exist, including viscous damping, viscoelastic damping, friction damping, and impact damping. Viscous and viscoelastic damping usually have a relatively strong dependence on temperature. Friction dampers, while applicable over wide temperature ranges, may degrade with wear. Due to these limitations, attention has been focused on impact dampers, particularly for application in cryogenic environments or at elevated temperatures.

Particle damping technology is a derivative of impact damping with several advantages. The literature typically distinguishes particle damping from impact damping based on the number and

---

*Tel.: +937-229-3022; fax: +937-229-4251.

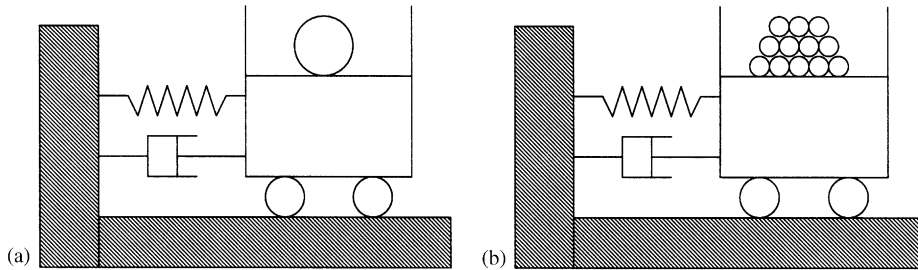*E-mail address:* olsonse@udri.udayton.edu (S.E. Olson).

Fig. 1. Idealized single-degree-of-freedom system with (a) impact damper and (b) particle damper.

sizes of the auxiliary masses (or particles) in a cavity. As shown in the idealized single-degree-of-freedom system in Fig. 1, impact damping usually refers to only a single (somewhat larger) auxiliary mass in a cavity, whereas particle damping is used to imply multiple auxiliary masses of small size in a cavity.

Particle dampers significantly reduce the noise and impact forces generated by an impact damper and are less sensitive to changes in the cavity dimensions or excitation amplitude. Studies conducted over recent years have demonstrated the effectiveness and potential application of particle dampers to reduce vibration in a space shuttle main engine liquid oxygen inlet tee [1] and to attenuate the resonant vibrations of antennae [2]. In recent years, a tennis racquet incorporating particle damping has even been introduced [3]. The behavior of particle dampers is highly non-linear with energy dissipation, or damping, derived from a combination of loss mechanisms. These loss mechanisms involve complex physical processes and cannot be analyzed reliably using current models. As a result, previous particle damper designs have been based on trial-and-error experimentation. A mathematical model has been developed which enables particle damper designs to be evaluated analytically. The model utilizes the particle dynamics method and captures the complex physics involved in particle damping.

2. Model development

The granular material in particle dampers is unique in that the material can display behavior similar to a solid, liquid, or gas, depending on the amount of energy contained in the material. Various techniques of modelling granular materials, including the particle dynamics method, have been proposed. The particle dynamics method is a method similar to that used to study molecular dynamics, where individual particles are modelled and their motions tracked in time. The procedure is an explicit process with sufficiently small time steps taken such that during a single time step, disturbances cannot propagate from any particle further than its immediate neighbors. As a result, at any given time, the resultant forces on any particle are determined exclusively by its interaction with the particles with which it is in contact. This feature makes it possible to follow the non-linear interaction of a large number of particles without excessive memory or the need for an iterative procedure.

The utility of the particle dynamics method is based on the ability to simulate contact interactions using a small number of parameters that capture the most important contact

properties. Interaction forces between the individual particles and the cavity walls are calculated based on force–displacement relations. Thus, one of the critical aspects for developing an accurate mathematical model is the selection of appropriate force–displacement relations to account for the forces created due to particle–particle and particle–cavity impacts.

In the mathematical model, it is assumed that the particle dampers consist of spherical particles of a single material. Consider a typical impact of two spherical particles, i and j, with radii R_i and R_j, with the particle centers separated by a distance, d_{ij}, as shown in Fig. 2. These two particles interact if their approach, α, is positive. The approach can be defined as

$$\alpha = (R_i + R_j) - d_{ij}. \tag{1}$$

In this case, the colliding spheres are subject to the contact force:

$$\vec{F} = F^N \cdot \vec{n}^N + F^S \cdot \vec{n}^S, \tag{2}$$

where F^N and F^S are the normal and shear forces and $\vec{n}^N$ and $\vec{n}^S$ are the unit vectors in the normal and shear directions, respectively, for a given sphere. The opposing sphere experiences equal forces in the opposite direction.

For purely elastic contacts, expressions for the normal force can be found from Hertz's theory of elastic contact [4,5]. For the case of two contacting spheres with identical properties, a circular contact area with radius, a, results. Hertz's expression for the normal force becomes
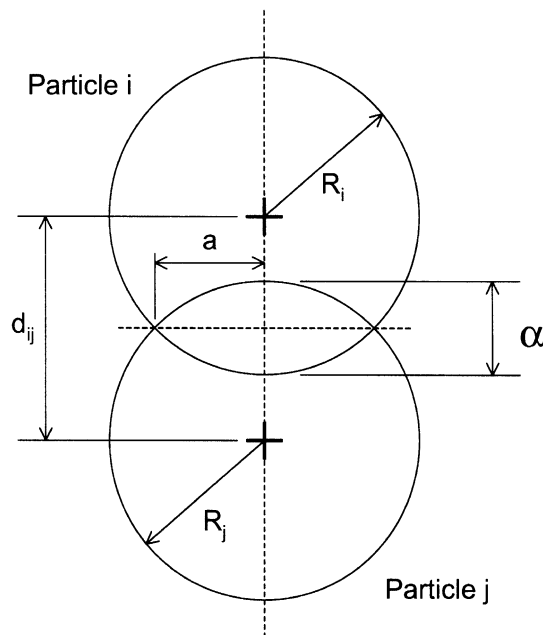
$$F^N = \frac{2}{3R}\frac{E}{(1 - v^2)}a^3, \tag{3}$$

Fig. 2. Typical particle–particle impact parameters

where

$$R = \frac{(R_i R_j)}{(R_i + R_j)} \tag{4}$$

and E and υ are the elastic modulus and the Poisson ratio of the spheres, respectively. The approach and contact circle radius are related as

$$\alpha = \frac{a^2}{R}. \tag{5}$$

Hertz's expression is for two contacting spheres, but also holds for two impacting spheres provided that the duration of the collision is long compared with the first fundamental mode of vibration in the spheres.

Typically, particle–particle impacts are not purely elastic and energy is dissipated during the impact event. For accurate damping predictions, it is important to incorporate this dissipation into the model. The enduring types of contacts which occur in the particle damper preclude the use of a coefficient of restitution or similar parameter. However, coefficient of restitution studies have demonstrated that energy is dissipated due to the viscoelastic behavior of the sphere material [6]. A three-parameter, generalized Maxwell model is used to represent the viscoelastic material, such that the relaxation function, $\Psi(t)$, takes the form

$$\Psi(t) = E_0 + E_1 e^{-t/\tau_1}. \tag{6}$$

Earlier work [6] indicates that, for hard metals and plastics, the dissipation due to the deviatoric and dilatational strains are of similar magnitudes. As a result, the relaxation function is not broken into separate deviatoric and dilatational components or, equivalently, it is assumed that the Poisson ratio remains constant.

Ideally, the dissipative portion of the normal force would be expressed in terms of a viscoelastic formulation of Hertz's theory. Lee and Radok [7] have shown that, as long as the contact area is increasing, a simple relation for the normal force can be derived by replacing the elastic modulus in Hertz's relation (Eq. (3)) with the relaxation function for the sphere material. Substituting the relaxation function into Hertz's relation and recognizing that the contact radius is also a function of time, the total normal force (i.e., the normal force due to the combined elastic and dissipative components) at any time can be expressed as

$$F^N(t) = \frac{2}{3R} \frac{1}{(1 - \upsilon^2)} \int_0^t \Psi(t - t') \frac{\mathrm{d}}{\mathrm{d}t'} a(t')^3 \, \mathrm{d}t'. \tag{7}$$

Substituting the relation in Eq. (5) for the contact radius, and the relation in Eq. (6) for the relaxation function yields

$$F^N(t) = \frac{R^{1/2}}{(1 - \upsilon^2)} \int_0^t \sum_{i=0}^n E_i e^{-(t-t')/\tau_i} \alpha(t')^{1/2} \dot{\alpha}(t') \, \mathrm{d}t', \quad \text{where } \frac{1}{\tau_0} = 0. \tag{8}$$

For greater utility, it would be beneficial to express Eq. (8) in incremental form such that state variables can be used to describe the loading at any time. By considering the individual contributions of each of the viscoelastic terms to the total normal force, the total force at any time

can be expressed as a summation of terms:

$$F^N(t) = \sum_{i=0}^{1} F_i^N(t). \tag{10}$$

With further rearrangement, and using the midpoint rule to evaluate the integral in Eq. (8), the following pair of incremental equations can be derived:

$$\text{for } i = 0: \quad F_0^N(t + \Delta t) = F_0^N(t) + \frac{R^{1/2}}{(1 - v^2)} E_0 \alpha(t + \Delta t/2)^{1/2} \dot{\alpha}(t + \Delta t/2)\Delta t, \tag{11}$$

$$\text{for } i = 1: \quad F_1^N(t + \Delta t) = F_1^N(t)e^{-\Delta t/\tau_1} + \frac{R^{1/2}}{(1 - v^2)} E_1 e^{-\Delta t/2\tau_1} \alpha(t + \Delta t/2)^{1/2} \dot{\alpha}(t + \Delta t/2)\Delta t. \tag{12}$$

The resulting relations are valid when the contact area is increasing, but break down late in the unloading due to negative (tensile) contact pressures which are predicted within the contact area. However, particle dampers typically contain metallic, ceramic, or hard plastic particles. For the relatively low levels of viscoelasticity in such particles, it is reasonable to impose the constraint that the total contact force becomes zero when a negative force is predicted. Note that these relations capture both the elastic and dissipative portions of the normal force and simplify to an incremental form of Hertz's relation when elastic properties are used.

In addition to normal forces, shear forces can be created when a particle slides along another particle or along the cavity walls, or when oblique impacts occur between individual particles or between particles and the cavity walls. Both slipping and non-slipping contact can occur. Of particular interest is the accurate representation of slipping contacts, as damping is created due to the dissipation of the heat generated by friction. When friction is introduced, the normal and shear forces interact. However, this interaction is generally small and it is typically assumed that the normal and shear forces are independent of each other [8]. This assumption is made in the present particle damper model.

The shear forces can be roughly divided into two classes of contact depending on the duration of the contact. The enduring type of contacts seen as a particle slides along another particle or along the cavity walls typically lasts significantly longer in time than the nearly instantaneous type of contacts seen during oblique impacts between individual particles or between particles and the cavity walls. As a result, the enduring contacts can have a much more significant effect on the overall damping than the oblique impacts, and it is important that the model accurately capture these effects.

For enduring contacts, the shear forces can be reasonably represented using Amonton's law of sliding friction (Coulomb friction) [8]:

$$F^S = -sgn(v_{rel}^t)\mu|F^N|, \tag{13}$$

where μ represents the particle–particle friction coefficient and v_{rel}^t is the relative tangential velocity. This relation suffers from two potential drawbacks: (1) when the slip rate is small, the shear force can rapidly change directions and create oscillations; and, (2) the relation is unable to capture static friction. However, the global motion of the system to be damped will likely prevent large oscillations in the shear force. In addition, static friction is not a concern since relative particle motion must occur for the particle damper to function. A single coefficient of friction is given, and it is assumed that particle motion occurs or that the static coefficient of friction is zero.

The Coulomb friction model also is used to account for the forces created due to the nearly instantaneous type of contacts seen during oblique impacts. Detailed finite element analyses show that this model generally performs well for higher angles of incidence (glancing impacts), but becomes less accurate at lower angles of incidence (closer to normal). However, in the particle damper model, it is more critical to accurately represent the enduring type of sliding contacts since these contacts generally last for a longer time and can have a more significant effect on the damping. Future enhancements to the particle damper model may include a more accurate representation of the shear forces generated during oblique impacts.

In addition to particle–particle impacts, particle–cavity impacts also occur and appropriate force–displacement relations are required. The particle–cavity force–displacement relations can be formulated by modifying the particle–particle relations to account for the material properties of the cavity and the local curvature. For simplicity, it has been assumed that the cavity walls are flat and rigid. Particle–cavity relations for flat cavity walls are derived from the particle–particle relations by assuming the radius of curvature for the cavity walls goes to infinity. Under the assumption of rigid walls, the effective modulus simply becomes the particle modulus.

The particle damper model has been implemented within X3D [9], an explicit finite element code developed to predict high-velocity impact events. The code contains various contact algorithms and bookkeeping routines and provides an appropriate framework for simulating particle damping through the use of the particle dynamics method. Particle–particle and particle–cavity contacts are resolved using the force–displacement relations discussed in the preceding paragraphs. Contact state variables are created when any contact event occurs, and are stored and updated throughout the course of that particular contact. Separate contact detection/resolution routines are used for particle–particle and particle–cavity contacts.

3. Application

To demonstrate and validate the particle damper model, testing and analysis of a cantilevered aluminum beam were performed. The beam was tested undamped and with various impact and particle dampers attached. The particle damper model was used to predict the behavior of the beam under various conditions.

The first flexural mode of a cantilevered aluminum beam was used for the laboratory testing. The beam was 304.8 mm in length, 38.1 mm wide, and 4.45 mm thick. The beam was rigidly fixed at the root and had a first flexural mode of slightly less than 40 Hz. The beam was excited near the root through a stinger attached to an electromagnetic shaker. Testing was performed with excitation signals of 200 mV RMS and 400 mV RMS input to the shaker. The excitation signal was held constant and, as a result, the peak forces near resonance were considerably less than those far from resonance. Accelerations were measured at the beam tip, with beam tip displacements calculated based on the assumption of true sinusoidal response.

Laboratory testing was performed on the undamped beam, on beams with added mass, and on beams damped with impact and particle dampers containing stainless steel spheres. The impact and particle damper cavities were constructed from square acrylic tubing with aluminum end caps epoxied to the tubing to enclose the cavities. For these tests, all of the impact and particle damper cavities were 9.45 mm wide, 9.45 mm high, and 6.68 mm long. Testing was performed on an
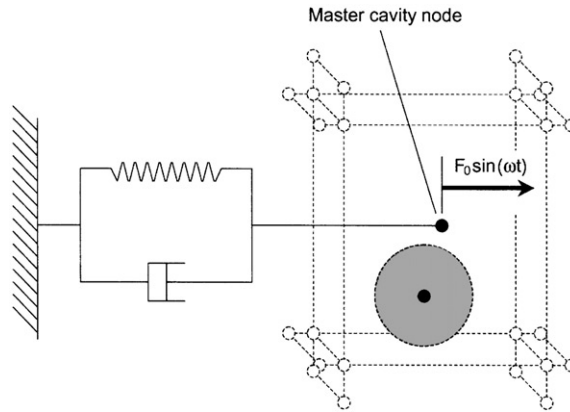
Fig. 3. Analytical model used to simulate particle dampers.

impact damper containing a single 6.35 mm diameter stainless steel sphere and on particle dampers containing 64 stainless steel spheres of 1.59 mm diameter and 512 stainless steel spheres of 0.79 mm diameter. These configurations were selected such that the total particle mass in each case was identical, eliminating any effects due solely to added mass.

Analytically, the beam used for the laboratory testing was modelled as a simple mass–spring–dashpot system as shown in Fig. 3. The beam was modelled as a lumped mass (at the master cavity node) attached to a damped spring-to-ground element. The equivalent mass and spring stiffness were chosen to simulate the first flexural mode of the undamped beam. The model captures the behavior at the beam tip; so initial estimates for the analytical drive force were based on the tip force equivalent to the measured force input near the root of the beam. Initial damping estimates were based on the measured loss factor from laboratory testing. The excitation force and damping were adjusted so that the predicted response of the undamped beam from the analytical simulations matched the undamped response measured experimentally. Thus, the analytical model was tuned for the undamped response. Subsequent damped analyses utilized the tuned model parameters. Unlike the laboratory testing, where the excitation signal to the shaker was held constant but the excitation force varied near resonance, the excitation force in the analyses was held constant for a given excitation level.

For damped simulations, the cavity was modelled using contact surfaces defined by nodes linked to the master cavity node. Particles were tracked using a node at the center of each particle. The particles initially were given a random distribution within the cavity and a gravity load was included to ensure that the particles pack on the bottom of the cavity. The mass of the particles was included based on the number of particles and the radius and density of each particle. Any additional mass due to the cavity was added to the equivalent mass of the undamped beam.

For the damper analyses shown here, the particles were given viscoelastic material properties with $E_0 = 189.6$ GPa, $E_1 = 34.5$ GPa, and $\tau_1 = 2.0\,\mu$s. These properties correspond to a maximum equivalent loss factor of 0.083 and an elastic modulus of 206.8 GPa at the frequency of the maximum loss factor. These properties were chosen based on restitution studies of a single sphere impacting a rigid plate. A coefficient of friction was given for the particles to account for the

frictional interactions between the individual particles or the particles and the cavity walls. A coefficient of friction of 0.30 was used in the analyses.

Fixed time steps were used in the simulations. The particle dynamics method requires that sufficiently small time steps be taken, so that during a single time step, disturbances cannot propagate from any particle further than its immediate neighbors. For these simulations, a time step of 0.5 μs was used. The simulations also must be performed to sufficiently long times, so that the steady state displacement of the cantilever beam can be determined. These simulations were run to a simulated time of 15.0 s, requiring solutions propagated through 30 million increments. Separate solutions were performed at each frequency of interest.

4. Results

Various simulations were performed corresponding to cases which were tested. Measurements were made on the undamped beam, the beam with an added mass equal to the mass of the dampers, and on various damper configurations (of the same total particle mass) containing one 6.35 mm diameter particle, 64, 1.59 mm diameter particles, and 512, 0.79 mm diameter particles. Fig. 4 shows experimental and analytical beam tip displacements at various frequencies for the
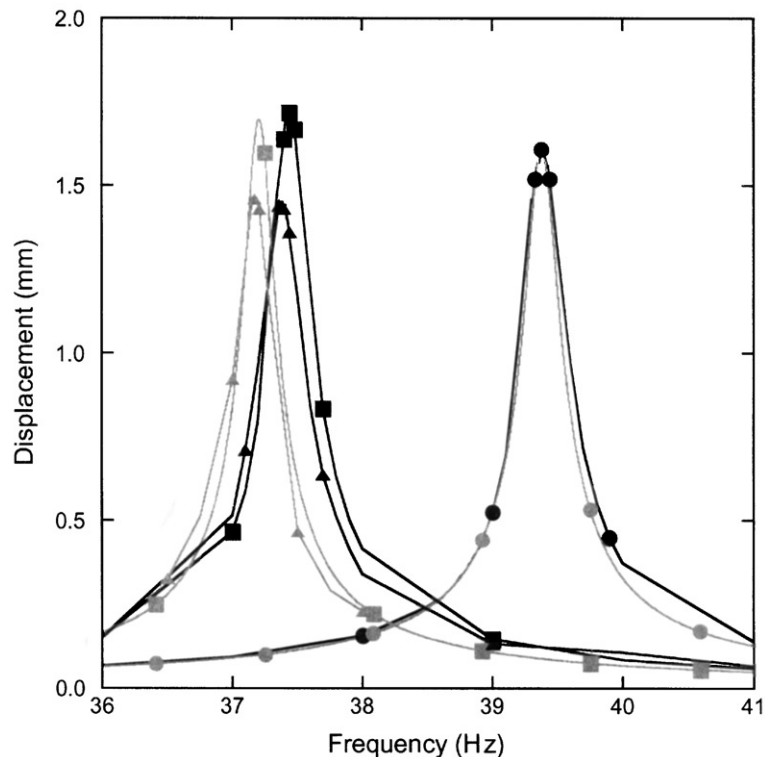
Fig. 4. Beam tip displacements under 200 mV RMS excitation force: undamped experiment, ●; undamped analysis, ◐; added mass experiment, ■; added mass analysis, ▨; one 6.35 mm diameter steel sphere experiment, ▲; one 6.35 mm diameter steel sphere analysis, ▴.
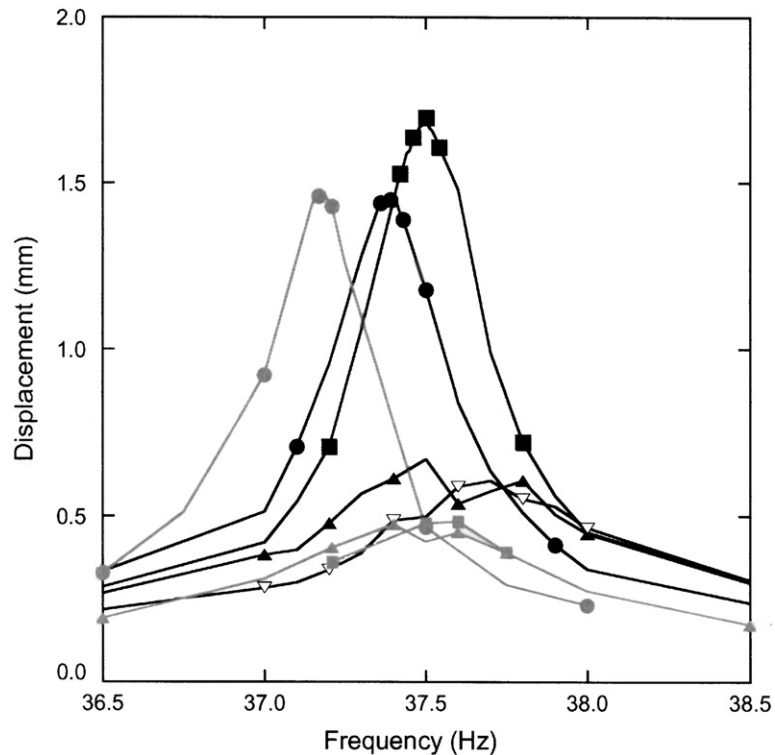
Fig. 5. Damped tip displacements under 200 mV RMS excitation force: one 6.35 mm diameter steel sphere experiment, ●; one 6.35 mm diameter steel sphere analysis, ●; 64, 1.59 mm diameter steel spheres experiment with increasing frequency, ▲; 64, 1.59 mm diameter steel spheres experiment with decreasing frequency, ▽; 64, 1.59 mm diameter steel spheres analysis, ▲; 512, 0.79 mm diameter steel spheres experiment, ■; 512, 0.79 mm diameter steel spheres analysis, ■.

undamped, added mass, and single-particle configurations under a force equivalent to a 200 mV RMS excitation signal to the shaker. Fig. 5 shows results for the various damped cases under a force equivalent to a 200 mV RMS excitation signal to the shaker. Similar results corresponding to a 400 mV RMS excitation signal to the shaker are shown in Figs. 6 and 7.

For some of the experimental results, two sets of data are given for the same configuration. In each case, the first set of results corresponds to data taken with the excitation frequency increasing during testing and the second set with the excitation frequency decreasing. The accelerations acting on the particles must become sufficiently large to overcome the forces of static friction or other cohesive forces. Once the friction or cohesive forces are overcome, the particles remain in motion until the excitation is removed. In the particle damper model, it is assumed that relative particle motion occurs. Therefore, the model will not capture any effects due to static friction or cohesive forces.

An interesting result is observed in the experimental data for the damper with 512 particles. At 200 mV RMS excitation, very little attenuation is seen. However, at 400 mV RMS excitation, considerable attenuation is observed once the displacements reach a certain level (whether the
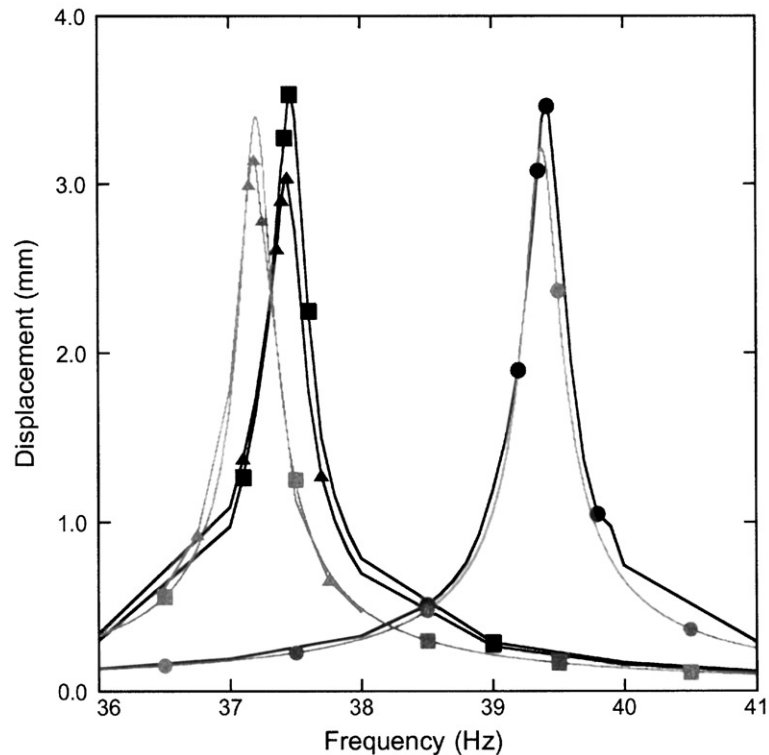
Fig. 6. Beam tip displacements under 400 mV RMS excitation force: undamped experiment, ●; undamped analysis, ●; added mass experiment, ■; added mass analysis, ■; one 6.35 mm diameter steel sphere experiment, ▲; one 6.35 mm diameter steel sphere analysis, ▲.

excitation frequency is increasing or decreasing). During laboratory testing, it was observed that there may be cohesive forces between the particles due to static electric charges or oil on the particles which influence the results.

In general, the particle damper model predicts the correct trends. For example, the model predicts little attenuation for the single-particle dampers, but considerably more attenuation for multiple-particle dampers containing 64 and 512 particles. The model also captures the experimental trend of optimum damping at a specific number of particles with less attenuation when either a lesser or a greater number of particles is used. This trend is evident in the increased attenuation observed when the number of particles is increased from a single particle to 64 particles, and the decreased attenuation observed when the number of particles is further increased to 512 particles. The model does tend to overpredict the attenuation, particularly for multiple-particle dampers. A portion of this discrepancy between the experimental and model data may be a result of controlling the shaker excitation signal for the laboratory testing, and controlling the actual excitation force in the analytical simulations. The model also does not capture any effects due to static friction or cohesive forces between the particles.
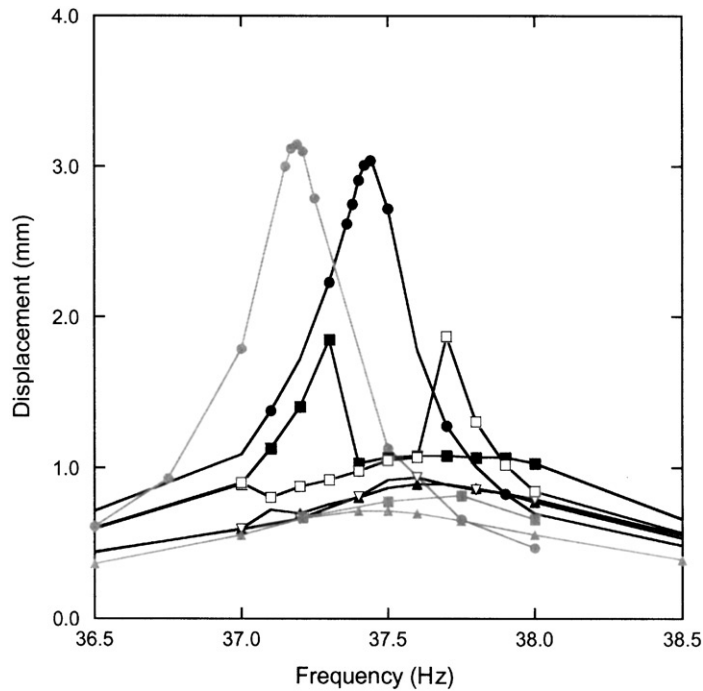
Fig. 7. Damped tip displacements under 400 mV RMS excitation force: one 6.35 mm diameter steel sphere experiment, ●; one 6.35 mm diameter steel sphere analysis, ●; 64, 1.59 mm diameter steel spheres experiment with increasing frequency, ▲; 64, 1.59 mm diameter steel spheres experiment with decreasing frequency, ▽; 64, 1.59 mm diameter steel spheres analysis, ▲; 512, 0.79 mm diameter steel spheres experiment with increasing frequency, ■; 512, 0.79 mm diameter steel spheres experiment with decreasing frequency, □; 512, 0.79 mm diameter steel spheres analysis, ■.

5. Conclusions

A mathematical model has been developed which allows particle damper designs to be evaluated analytically. The model is based on the particle dynamics method and adequately captures the complex physical interactions that occur in particle dampers. Application of the model has been demonstrated by simulating laboratory testing of a cantilevered beam. Model predictions generally compare well with test results. It is anticipated that future enhancements to the model will further improve the correlation.

References

[1] H.V. Panossian, Structural damping enhancement via non-obstructive particle damping technique, Journal of Vibration and Acoustics 114 (1992) 101–105.

[2] S.S. Simonian, Particle beam damper, Proceedings of the SPIE 2445 (1995) 149–160.

[3] S. Ashley, A new racket shakes up tennis, Mechanical Engineering 117 (1995) 80–81.

[4] H. Hertz, Über die Berührung fester elastischer Körper (On the contact of elastic solids), Journal für die reine und angewandte Mathematik 92 (1881) 156–171 (for English translation see in: D.E. Jones, G.A. Schott (Eds.), Miscellaneous Papers by Heinrich Hertz, MacMillan, New York, NY, 1896).

[5] H. Hertz, Über die Berührung fester elastischer Körper und über die Härte (On the contact of rigid elastic solids and on hardness), Verhandlungen des Vereins zur Beförderung des Gewerbefleisses (1882) (for English translation see in: D.E. Jones, G.A. Schott (Eds.), Miscellaneous Papers by Heinrich Hertz, MacMillan, New York, NY, 1896).

[6] G. Kuwabara, K. Kono, Restitution coefficient in a collision between two spheres, Japanese Journal of Applied Physics 26 (1987) 1230–1233.

[7] E.H. Lee, J.R.M. Radok, The contact problem for viscoelastic bodies, Journal of Applied Mechanics 27 (1960) 438–444.

[8] K.L. Johnson, Contact Mechanics, Cambridge University Press, New York, 1985.

[9] R.A. Brockman, T.W. Held, Technical Report UDR-TR-92-59, X3D User's Manual, University of Dayton Research Institute, 1994.